



Effect of pretreating technologies on the adhesive strength and anticorrosion property of Zn coated NdFeB specimens

Pengjie Zhang^{a,b,c,d}, Guangqing Xu^{a,*}, Jiaqin Liu^a, Xiaofei Yi^{a,b,c,d}, Yucheng Wu^{a,*}, JingWu Chen^{b,c,d}

^a School of Materials Science and Engineering, Hefei University of Technology, Hefei 230009, China

^b Earth-Panda Advance Magnetic Material Co. Ltd., Hefei, China

^c Anhui Province Key Laboratory of Rare Earth Permanent Magnet Materials, Hefei, China

^d State Key Laboratory of Rare Earth Permanent Magnet Materials (Earth-Panda Advance Magnetic Material Co., Ltd.), Hefei, China



ARTICLE INFO

Article history:

Received 17 September 2015

Received in revised form 6 December 2015

Accepted 10 December 2015

Available online 12 December 2015

Keywords:

Pretreating technology

Zn coating

NdFeB specimen

Adhesive strength

Anticorrosion property

ABSTRACT

Zinc coated NdFeB specimens were prepared with different pretreating technologies, such as polishing, pickling (50 s), sandblasting and combined technology of sandblasting and pickling (5 s). Morphologies of the NdFeB substrates pretreated with different technologies were observed with a scanning electron microscope equipped with an energy dispersive spectrometer and an atomic force microscope. The tensile test was performed to measure the adhesive strength between Zn coating and NdFeB substrate. The self-corrosion behavior of the NdFeB specimen was characterized by potentiodynamic polarization curve. The anticorrosion properties of Zn coated NdFeB specimens were characterized by neutral salt spray tests. The pretreating technologies possess obvious impact on the adhesive strength and anticorrosion property of Zn coated NdFeB specimens. Combined pretreating technology of sandblasting and pickling (5 s) achieves the highest adhesive strength (25.56 MPa) and excellent anticorrosion property (average corrosion current density of 21 $\mu\text{A}/\text{cm}^2$) in the four pretreating technologies. The impacting mechanisms of the pretreating technology on the adhesive strength and anticorrosion properties are deeply discussed.

© 2015 Published by Elsevier B.V.

1. Introduction

Sintered NdFeB permanent magnet is widely used in various industries, such as electronics, communications, medical apparatus and airplane industries, due to its remarkable magnetic property [1–4]. However, poor corrosion resistance of the magnet restricts its application in high temperature and humid environments [5–7]. The main reason for low corrosion resistance of the NdFeB is the negative electrochemical potential (Generally, the free corrosion potential of sintered NdFeB specimen in neutral solution is approximate $-0.75 \pm 0.05 \text{ V}_{\text{SCE}}$) [8,9] and the multi-phase structure of sintered NdFeB [9,10]. The microstructure of NdFeB permanent magnet comprises of ferromagnetic matrix-phase ($\text{Nd}_2\text{Fe}_{14}\text{B}$) surrounded by B-rich ($\text{Nd}_{1+x}\text{Fe}_4\text{B}_4$) and Nd-rich (Nd_4Fe) phases. Other beneficial phases stabilized by alloying additions such as Al, Co, Cu, Cr, Mo, Nb and Ga may also be present [11]. The existence of magnet phases with large electrochemical potential differences presents an obvious threat of galvanic corrosion [12]. Many efforts

have been applied to improve the corrosion resistance of NdFeB magnet, such as alloy additions [13–15] and surface treatments [16–26]. By adding alloy elements, such as Al [13], Co [15], Cu and Ga [14], the corrosion resistance of the magnet has been promoted greatly. However, this promotion is at the expense of decreasing the magnetic performance of NdFeB magnet. Surface coating technologies are the mostly used methods for promoting corrosion resistance, including metal coatings [16–22] and organic coatings [23–26]. Among the surface coating technologies, electroplated coatings have been widely used due to low cost, easy to operate and industrialized production [16,19–22].

However, the sintered NdFeB magnet is a powder-metallurgical material, and there are many cracks and micropores in the magnets [27,28]. In the traditional electroplate pretreating process, pickling in 5% HNO_3 solution for 40–80 s was the main rust removal technique due to the convenient industrialization implementation [28,29]. However, the acid solution not only leads to the corrosion of the rust on the substrate, but also remains in the cracks and micropores of the magnet, resulting in the failure of the electroplated coatings. Furthermore, the surface layer of the substrate is a loose layer after pickling process, resulting in the decrease of the adhesive strength between the coating and substrate [29].

* Corresponding authors. Tel.: +86 551 62901012; fax: +86 551 62901362.

E-mail addresses: gqxu1979@hfut.edu.cn (G. Xu), ycwu@hfut.edu.cn (Y. Wu).

Sandblasting technology attracted increasing attentions as an environment friendly method [30–32], which can avoid the magnet corrosion and increase the surface roughness which is benefit to the adhesive strength between the coating and substrate [33–35]. However, the production efficiency of the sandblasting technology is a little lower than that of pickling process. Polishing is also a rust removal technique used in NdFeB substrate pretreating process. However, the production efficiency is the lowest among the three technologies due to the absence of specialized industrial equipment. Hence, this technology is always used in the laboratory.

The pickling process has been deeply studied in the past twenty years [28,29]. However, little work has been reported on the sandblasting process applying as rust removal technique on sintered NdFeB. Here, polishing, pickling (50 s), sandblasting and combined technology of sandblasting and pickling (5 s) were used as pretreating technologies for the following Zn coating, and the effect of different pretreatments on the adhesive strength and anticorrosion property of Zn coated NdFeB specimens were discussed.

2. Experimental details

2.1. Pretreating process

NdFeB specimens ($(\text{PrNd})_{25.6}\text{Dy}_{9.8}\text{Fe}_{\text{bal}}\text{B}_1\text{M}$, N42UH, Anhui Earth-Panda Advance Magnetic Material Co. Ltd.) were fabricated with the sintering method by industry manufacturer. All specimens were in the state of demagnetization. The specimens were cut into $30\text{ mm} \times 30\text{ mm} \times 3\text{ mm}$ for adhesive strength test and $10\text{ mm} \times 10\text{ mm} \times 5\text{ mm}$ for anticorrosion property measurements.

Four different pretreating techniques were used for the above-mentioned NdFeB substrates. (1) Polishing: The specimens were successively grinded with SiC abrasive paper from 200# to 1200#, and then ultrasonically cleaned in ethanol and deionized water; (2) Pickling (50 s): The samples were dipped into a 3% NaOH solution for 10 s and in 5% nitric acid solution for 50 s at room temperature, then rinsed with acetone and distilled water successively; (3) Sandblasting: The samples were put in the sandblasting machine, and 100 μm glass sand was used as the blasting media. The distance and jet angle between spray nozzle and the sample were 5 cm and 60°, respectively. The pressure of the spray gun was 0.8 MPa, and the duration time was 2 min. The specimens were rinsed with acetone and distilled water successively after being sandblasted; (4) Combined technology of sandblasting and pickling (5 s): The samples were sandblasted for 2 min and pickled in 5% nitric acid solution for 5 s, respectively.

2.2. Zn electroplating process

All NdFeB substrates were dipped into a citric acid for 15 s, and then put into the plating tank. The composition and other

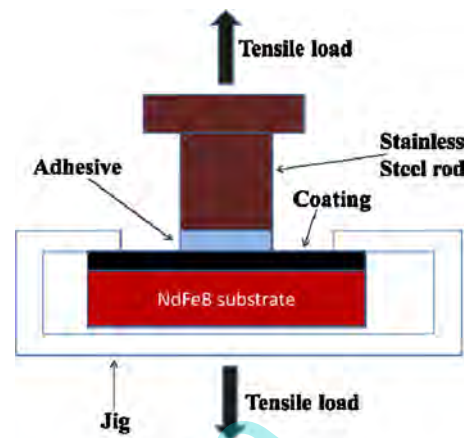


Fig. 1. Schematic diagram of testing adhesive strength.

parameters for the electroplating of Zn coating are given in Table 1. All the reagents are of analytical grade.

2.3. Characterization

The surface and cross-section morphologies of pretreated substrates were observed by a scanning electron microscope (SEM, JEOL JSM-6300F) equipped with an energy dispersive spectrometer (EDS). An atomic force microscope (AFM, CPM5500A) was used to analyze the surface roughness of the different pretreated samples. The adhesive strength between Zn coating and NdFeB substrate was characterized by vertical tensile test [36]. An electronic universal testing machine (WDW-20, Jinan Shidai Assaying Instrument Co. Ltd.) was used to measure the adhesive strength. The schematic diagram of the test mount is shown in Fig. 1. The test areas of the all specimens are 572.55 mm^2 (calculated by radius of 13.5 mm). E-7 glue (bonding strength of 70 MPa) was used as the adhesives. A stainless steel rod with diameter of 27 mm was glued onto the coating followed with airing at room temperature over 72 h. Then a groove was made surrounding the steel rod to cut the contacted area off from other area. Load-displacement curve was recorded with the increase of tensile load until the coating was stripped out from the NdFeB substrate. The adhesive strength is calculated by equation of $S = L_{\max}/A$, where S is the adhesive strength (unit: Pa), L_{\max} is the maximum load value (unit: N). A is the contact area between the stainless steel rod and the coating (unit: m^2). 10 tensile samples were carried out for the adhesive strength test for each pretreating condition.

The self-corrosion behaviors of NdFeB substrates with different pretreating technologies were measured with electrochemical potentiodynamic polarization. The anticorrosion properties of Zn coated NdFeB specimens with different pretreating technologies were measured with neutral salt spray (NSS) tests, and 5 samples were carried out for the NSS test for each pretreating condition. The electrochemical tests were conducted using a Potentiostat/Galvanostat (Autolab, Ecochimie) with a classical three electrode system comprising of a saturated calomel reference electrode (SCE), platinum sheet counter electrode and the samples as working electrode (exposed surface of 1 cm^2). The corrosion electrolyte used in all corrosion tests was 3.5 wt% sodium chloride (NaCl) solution at $25 \pm 3^\circ\text{C}$. Before the test, the specimens were immersed in the NaCl solution for 5 min to obtain the stationary potential. The NSS test was performed in a standard salt spray cabinet with spraying NaCl solution of 50 g/dm^3 at $35 \pm 2^\circ\text{C}$. The evolution of the corrosion phenomena was observed up to 9 days.

Table 1

Bath compositions and operating conditions for electroplating.

Bath compositions and operating conditions	Value
ZnCl ₂	30 g/L
NH ₄ Cl	200 g/L
(NH ₂) ₂ CS	2 g/L
CH ₃ COOH	120 mL/L
SDS	0.2 g/L
Current density	5 A/cm ²
Temperature	25 °C
pH	4.5
Time	30 min

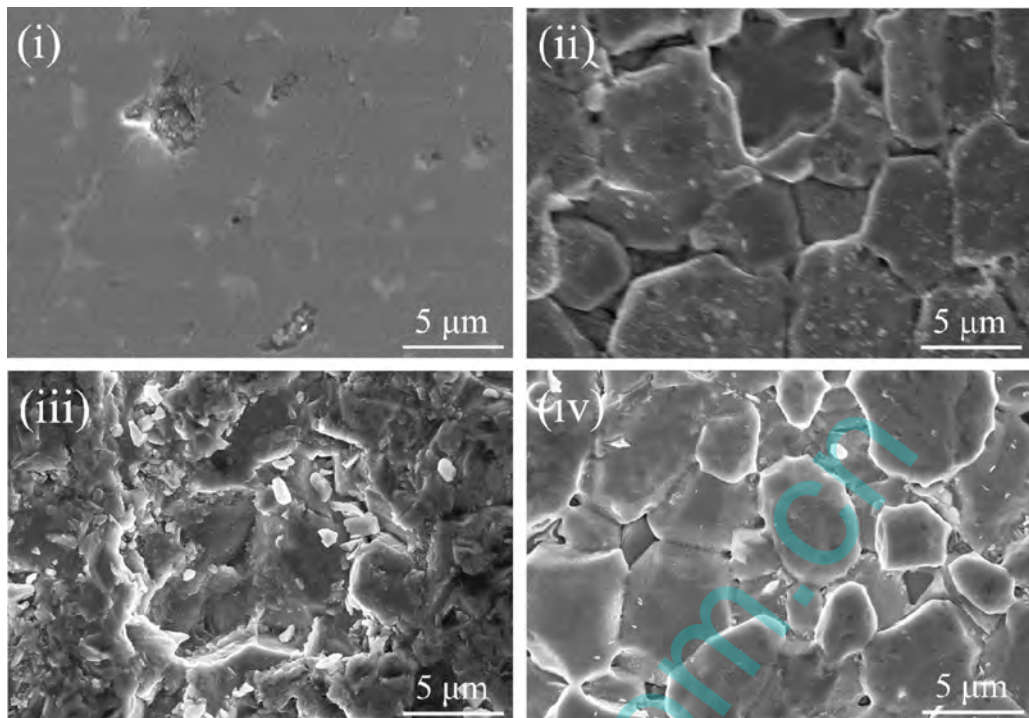


Fig. 2. SEM morphologies (SE mode) of NdFeB substrates with different pretreating technologies, (i) Polishing, (ii) Pickling (50 s), (iii) sandblasting and (iv) combined technology of sandblasting and pickling (5 s).

3. Results and discussion

3.1. Characterizations

Fig. 2 shows SEM morphologies of NdFeB substrates with different pretreating technologies of (i) polishing, (ii) pickling (50 s), (iii) sandblasting and (iv) combined technology of sandblasting and pickling (5 s). The polished substrate is smooth in surface, as shown in **Fig. 2(i)**. As shown in **Fig. 2(ii)**, the ferromagnetic matrix-phase grains of the NdFeB substrates are bulgy after been pickled for 50 s. The intergranular regions and grain boundary intersection corner possess big and clear cracks and voids, indicating the dissolution of Nd-rich phases in the intergranular regions by nitric acid solution in the pickling process.

The surface of the specimen after being sandblasted becomes rough and uneven, and many small broken particles exist on the surface, as shown in **Fig. 2(iii)**. The loose structure induced by the broken particles is harmful for the following electroplating. Compared with the substrates pretreated with sandblasting and pickling (50 s) technologies, no broken particles and evident cracks can be observed on the substrate pretreated with combined technology of sandblasting and pickling (5 s), as shown in **Fig. 2(iv)**. However, there are some voids in the grain boundary intersection corner, indicating that the Nd-rich phases on the grain boundary intersection corner are firstly dissolved in nitric acid solution.

Fig. 3 shows the backscattered electron images of NdFeB substrates with different pretreating technologies, (i) polishing, (ii) pickling (50 s), (iii) sandblasting and (iv) combined technology of sandblasting and pickling (5 s). As shown in **Fig. 3(i)**, the evident white part in intergranular regions among the ferromagnetic matrix-phase grains can be observed to be Nd-rich phase [10]. However, after being pickled for 50 s, only single ferromagnetic matrix-phase can be observed on the surface layer of substrate, as shown in **Fig. 3(ii)**. The cracks and voids instead of Nd-rich phase appears in the intergranular regions indicate the dissolving of Nd-rich phase during pickling process.

Fig. 3(iii) shows the backscattered electron image of NdFeB substrate pretreated by sandblasting. No clear grain boundary can be observed due to the broken particles covering on the surface, which cannot be removed by ultrasonic cleaning. The existence of white Nd-rich phase indicates there is no selective removal of Nd-rich phase during sandblasting process.

Fig. 3(iv) shows the backscattered electron image of NdFeB substrate pretreated by the combined technology of sandblasting and pickling (5 s). Compared with single sandblasting pretreatment, the relatively clear grain boundary can be observed on the substrate, indicating that the broken particles can be removed by the pickling process. Compared with singe pickling technology, the cracks and void in the intergranular regions are much smaller, indicating the smaller damage to the substrate during the combined pretreating process due to the short pickling time.

Fig. 4 shows the backscattered electron images of profile view of Zn coated NdFeB specimens with different pretreating technologies, (i) polishing, (ii) pickling (50 s), (iii) sandblasting and (iv) combined technology of sandblasting and pickling (5 s). **Fig. 4(i)** shows the profile image of Zn coated NdFeB specimen pretreated with polishing. The interface between the coating and NdFeB substrate is relative straight with coating thickness of 4.3 μm. The Nd-rich phase in the substrate can be differentiated as the white part, and cannot be removed selectively in the polishing process. **Fig. 4(ii)** shows the profile image of Zn coated NdFeB specimen pretreated with pickling (50 s) process. The intergranular Nd-rich phases were removed in the surface layer of substrate. Also, Micro-cracks along the grain boundary can be observed in this area, which may be ascribed to the dissolution of the Nd-rich phases in the grain boundary in the acid solution, resulting in the loose structure in the surface layer of the substrate [28,29] after being pickled for 50 s. When pretreated with sandblasting technology, there is a broken-grain layer in the surface layer of the substrate, and Zn coating is deposited on these broken particles, as shown in **Fig. 4(iii)**. Nd-rich phases are still remained in the broken grain layer without selective removal. The other thing should be noted is that the Zn coating on

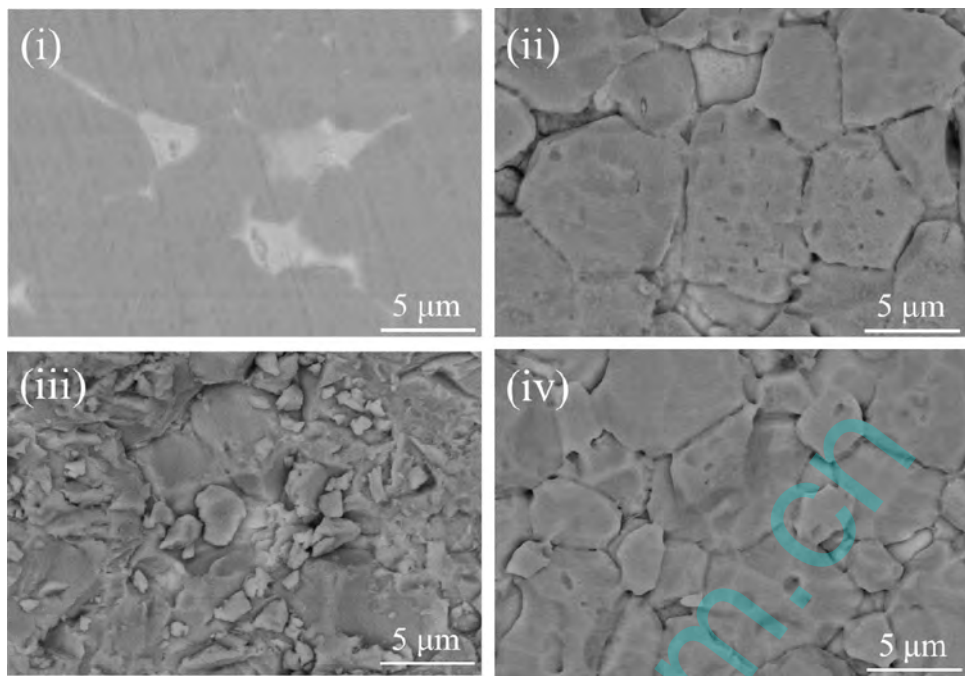


Fig. 3. Backscattered electron images of NdFeB substrates with different pretreating technologies, (i) Polishing, (ii) Pickling (50 s), (iii) sandblasting and (iv) combined technology of sandblasting and pickling (5 s).

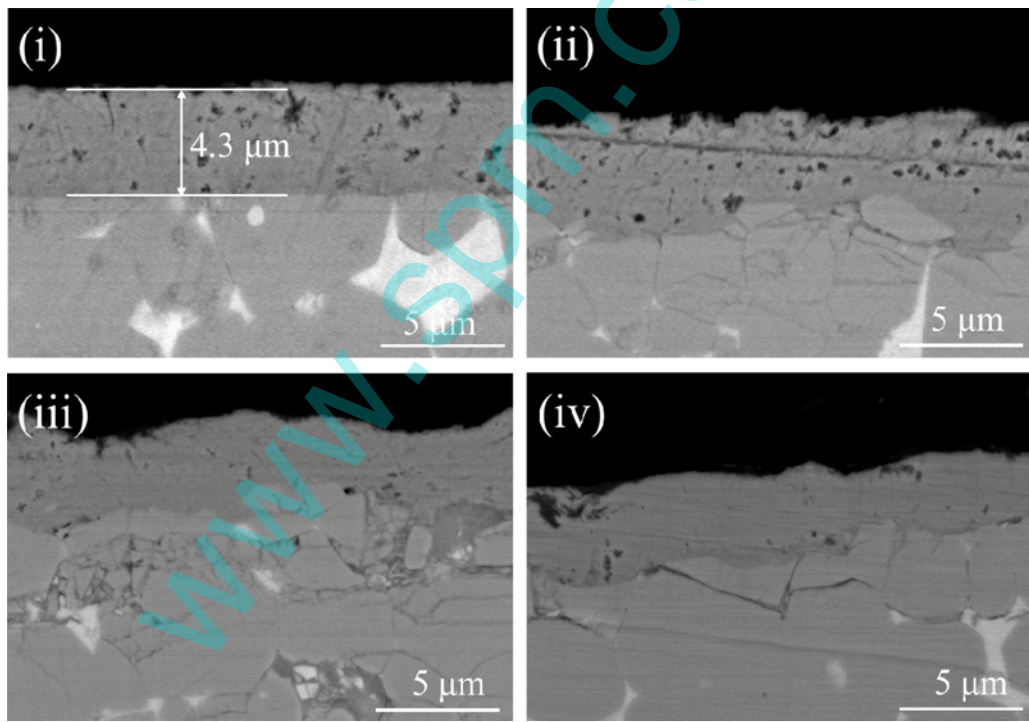


Fig. 4. The cross-sectional backscattered electron images (BSE mode) of Zn coated NdFeB substrates with different pretreating technologies, (i) Polishing, (ii) Pickling (50 s), (iii) sandblasting and (iv) combined technology of sandblasting and pickling (5 s).

the sandblasted substrate is much denser than that on the polished and pickled substrate, which may be due to the higher surface activity of the sandblasted substrate. Fig. 4(iv) shows the profile image of Zn coated NdFeB specimen pretreated with combined technology of sandblasting and pickling (5 s). No broken particles and micro cracks can be observed in the surface layer of the substrate, and the Nd-rich phases have been partly removed due to the pickling technology. Also, the Zn coating is as dense as the sandblasting

sample. The combined effects of the two technologies, such as low amount of Nd-rich phase, compact surface of the substrate and the dense coating, are benefit for enhancing the adhesive strength and anticorrosion properties of Zn coated NdFeB specimens.

Energy Dispersive Spectrometer (EDS) was performed to investigate the elemental compositions of NdFeB substrates pretreated with different technologies, and the results are shown in Table 2. The total contents of rare earth elements in the substrates

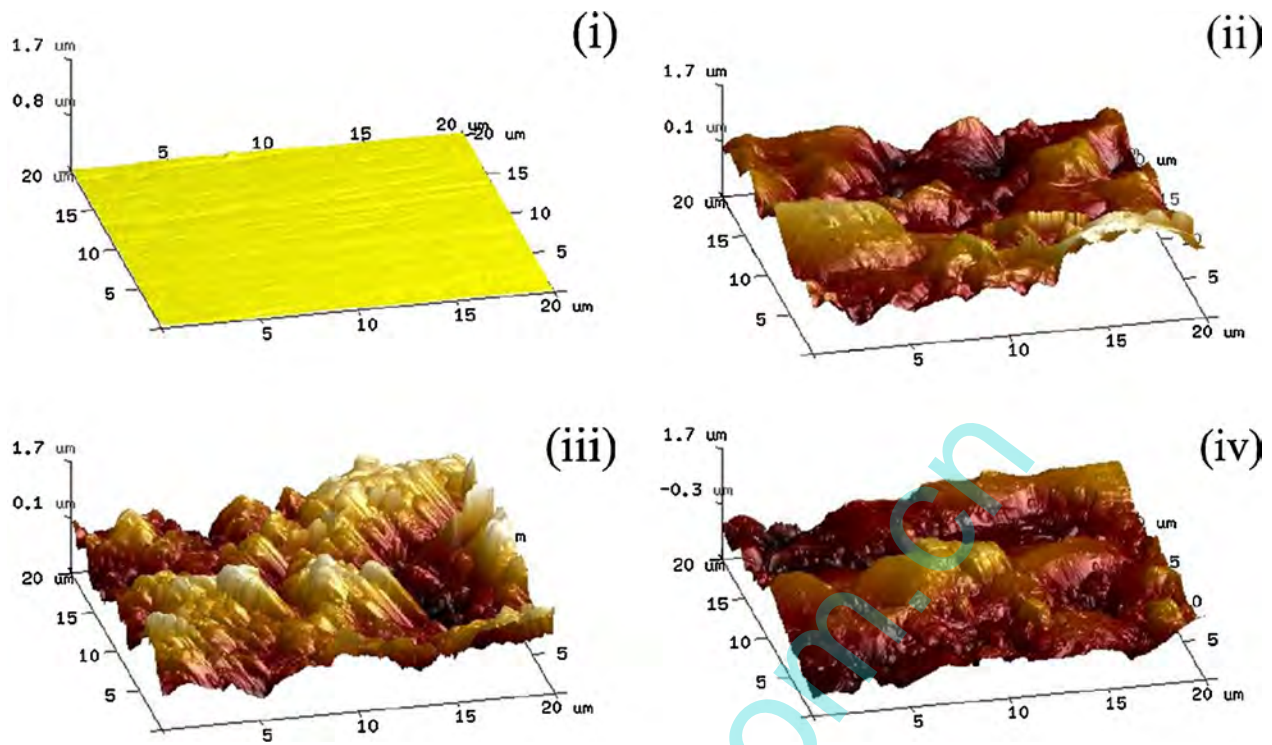


Fig. 5. AFM images of NdFeB substrates with different pretreating technologies, (i) polishing, (ii) pickling (50 s), (iii) sandblasting and (iv) combined technology of sandblasting and pickling (5 s).

Table 2
EDS analysis of NdFeB substrates pretreated with different technologies.

Pretreating technology	Nd (%)	Dy (%)	Pr (%)	$\sum \text{Re} (\%)$
Polishing	18.8 ± 0.2	9.6 ± 0.3	6.8 ± 0.2	35.3 ± 0.4
Pickling (50 s)	18 ± 0.3	8 ± 0.3	5.3 ± 0.3	31.3 ± 0.6
Sandblasting	18.9 ± 0.3	10.1 ± 0.2	6.2 ± 0.3	35.2 ± 0.6
Sandblasting + pickling (5 s)	18.5 ± 0.2	8.1 ± 0.2	4.8 ± 0.3	31.4 ± 0.6

pretreated with polishing, pickling (50 s), sandblasting and combined technology of sandblasting and pickling (5 s) are 35.3%, 31.3%, 35.2% and 31.4%. The total contents of rare earth of the substrates pretreated with pickling (50 s) and combined technology of sandblasting and pickling (5 s) are lower than that of polishing and sandblasting substrates with the decrement of approximate 4%, which can be ascribed to the dissolution of Nd-rich phases during pickling process. Considering the segregation of Dy and Pr in the intergranular regions, the decreases of Dy and Pr contents are even more obvious than that of Nd.

Fig. 5 shows the three-dimensional AFM images of NdFeB substrates with different pretreating technologies, (i) polishing, (ii) pickling (50 s), (iii) sandblasting and (iv) combined technology of sandblasting and pickling (5 s). Only the surface of the polishing substrate is smooth, as shown in Fig. 5(i). The other three substrates possess uneven surface in Fig. 5(ii)–(iv). The roughness data, including average roughness R_a and root mean square roughness R_q , of NdFeB substrates pretreated with different technologies are listed in Table 3. The polishing substrate possesses a smooth surface with the lowest average roughness value of 8.34 nm. The other three substrates possess much higher roughness value than that of polished substrate, such as 304 nm for pickling substrate, 409 nm for sandblasting substrate and 379 nm for the substrate pretreated with combined technology of sandblasting and pickling (5 s).

Table 3
Surface roughness values of NdFeB substrates pretreated with different technologies.

Specimens	R_a (nm)	R_q (nm)
Polishing	8.34 ± 2	10.9 ± 1.5
Pickling (50 s)	304 ± 13	373 ± 11
Sandblasting	409 ± 21	506 ± 16
Sandblasting + pickling (5 s)	379 ± 14	465 ± 7

3.2. Adhesive strength

Tensile test was performed to characterize the adhesive strength between Zn coating and NdFeB substrates with different pretreating technologies, and the results are shown in Fig. 6. Fig. 6(i) shows the typical tension–displacement curves of Zn coated NdFeB specimens with different pretreating technologies. The average adhesive strengths of Zn coated NdFeB specimens with error bars are shown in Fig. 6(ii). The average adhesive strengths of the Zn coated NdFeB specimens with pretreating technologies of polishing, pickling (50 s), sandblasting and combined technology of sandblasting and pickling (5 s) are 14.04, 18.98, 9.02 and 26.56 MPa, respectively. Both the adhesive strengths of specimens pretreated with pickling and combined technology of sandblasting and pickling (5 s) are higher than that of polishing sample due to the higher roughness. The adhesive strength between the coating and substrate will increase with the roughness in a certain range.

There are two reasons which can illustrate this phenomenon. On one hand, high roughness of the substrate will produce high hook chain and riveting effects between the coating and substrate. Fig. 7 shows the schematic diagram of the relationship between surface roughness of NdFeB substrate and adhesive strength of Zn coating. Zn particles will nucleate in an uneven region on the substrate surface firstly, and then grow up to be a complete coating during the electroplating process. High roughness increases the hook

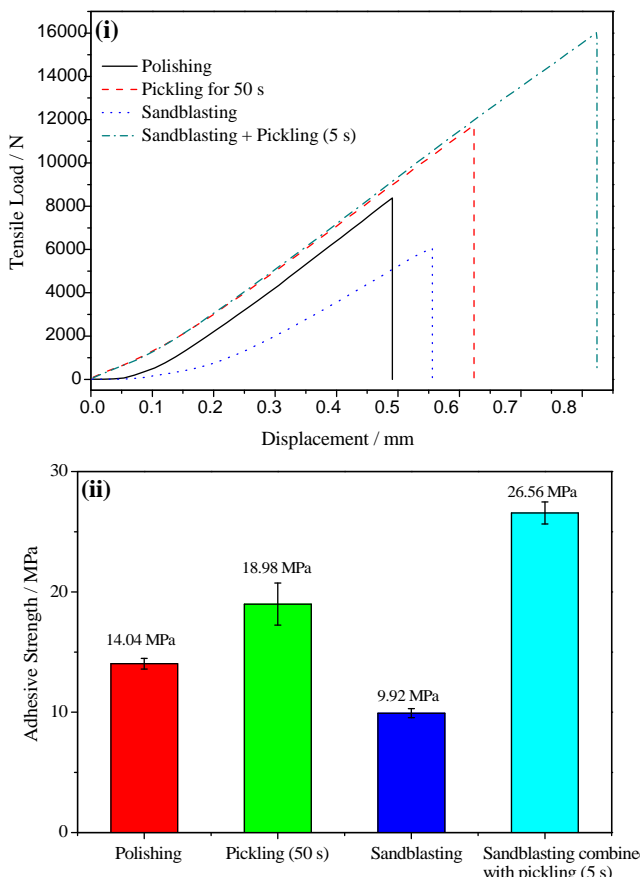


Fig. 6. Typical tensile load–displacement curves (i) and average adhesive strengths (ii) between Zn coatings and NdFeB substrates with different pretreating technologies.

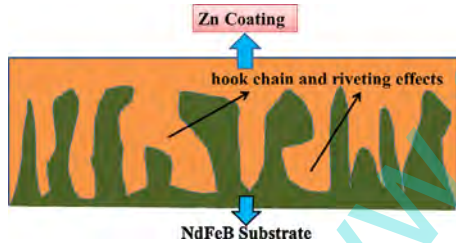


Fig. 7. Schematic diagram of the relationship between the surface roughness and the adhesive strength.

chain and riveting effects between the coating and substrate, hence enhances the adhesive strength between Zn coating and NdFeB substrate. On the other hand, the real surface area will increase with the increase of roughness, which produces higher contact area between Zn coating and the substrate [37].

However, the average adhesive strength of the sandblasting samples is only 9.02 MPa, although they possess the maximum surface roughness. As shown in Figs. 3(iii) and 4(iii), there are many broken particles and damaged grains observed on the surface of the sandblasting substrate forming a damaged layer, which cannot be removed with the following ultrasonic cleaning. The existence of the broken particles results in the low adhesive strength between Zn coating and the substrate.

Although the damaged layer cannot be eliminated through prolonging the ultrasonically cleaning time, it's easy to be removed by pickling in a short time. When the sandblasting substrate is pickled in nitric acid solution for 5 s, the damaged grains can react with the nitric acid quickly and the broken particles can be removed

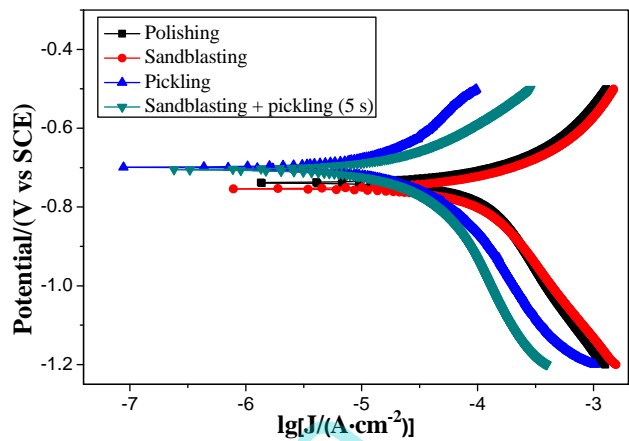


Fig. 8. Polarization curves of NdFeB substrates with different pretreating technologies in 3.5% NaCl solution.

Table 4

Electrochemical parameters calculated from the polarization curves.

Pretreating technology	E_{corr} (V vs. SCE)	I_{corr} (A/cm^2)
Polishing	-0.7406 ± 0.0024	$1.087 \pm 0.15 \times 10^{-4}$
Pickling (50 s)	-0.6991 ± 0.0037	$2.155 \pm 0.92 \times 10^{-5}$
Sandblasting	-0.7559 ± 0.0051	$1.213 \pm 0.27 \times 10^{-4}$
Sandblasting + pickling (5 s)	-0.7073 ± 0.0042	$2.180 \pm 1.17 \times 10^{-5}$

thoroughly, as shown in Figs. 3(iv) and 4(iii). The loose layer won't form on the substrate due to the low pickling time of 5 s. Therefore, the combined pretreating technology of sandblasting and pickling (5 s) produce the highest adhesive strength between Zn coating and substrate.

3.3. Corrosion property of the Zn plating

3.3.1. Potentiodynamic polarization curves

The potentiodynamic polarization curves of different pretreated NdFeB substrates were measured after being immersed in a 3.5 wt% NaCl solution for 5 min, as shown in Fig. 8. The corrosion potential (E_{corr}) and corrosion current density (I_{corr}) of the four specimens are listed in Table 4. The corrosion potentials of NdFeB substrates pretreated with different technologies of polishing, pickling (50 s), sandblasting and combined technology of sandblasting and pickling (5 s) are -0.7406 , -0.6991 , -0.7559 and -0.7073 V, respectively. The change of the corrosion potential reflects the thermodynamic tendency of corrosion. Higher corrosion tendency of polishing and sandblasting substrates can be obtained due to more negative corrosion potential of polishing and sandblasting pretreated substrates (-0.7406 and -0.7559 V) than that of substrates pretreated with pickling (50 s) and combined technology. That is, the substrates pretreated with pickling and combined technologies possess higher anticorrosion properties.

The corrosion currents of NdFeB substrates pretreated with different technologies of polishing, pickling (50 s), sandblasting and combined technology of sandblasting and pickling (5 s) are 1.087×10^{-4} , 2.155×10^{-5} , 1.213×10^{-4} and 2.180×10^{-5} A/cm², respectively. Low corrosion currents of substrates pretreated with pickling and composite technology of sandblasting combined with pickling (5 s) indicate high anticorrosion property, which corresponds with the results of corrosion potential.

According to the Faraday law, the relationship between corrosion rate and corrosion current density is as follows [38]:

$$\nu = \frac{MI_{corr}}{nF}$$

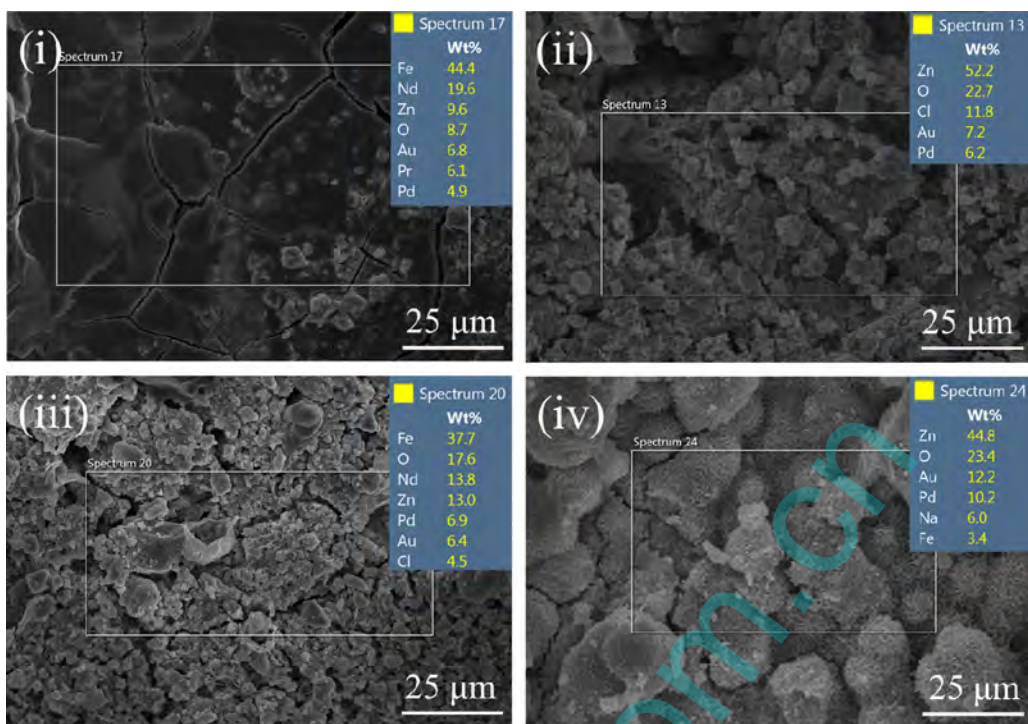


Fig. 9. SEM morphologies (SE mode) and EDS elemental compositions of Zn coated NdFeB specimens with different pretreatments after 132 h NSS test, (i) polishing, (ii) pickling (50 s), (iii) sandblasting and (iv) combined technology of sandblasting and pickling (5 s).

where v is corrosion rate, M is the atomic weight of corrosion metal, n is the chemical valence state and F is Faraday's constant. The corrosion rate is proportional to the corrosion current density. Considering solely the results of potentiodynamic polarization curves, the anticorrosion properties of substrates pretreated with pickling (50 s) and sandblasting combined with pickling (5 s) are better than that of polishing and sandblasting pretreated substrates.

3.3.2. Neutral salt spray test

The NSS test was performed to investigate the anticorrosion properties of Zn coated NdFeB specimens pretreated with different technologies of polishing, pickling (50 s), sandblasting and combined technology of sandblasting and pickling (5 s), respectively. In each pretreating condition, 5 samples were tested at the same time to reduce the test error. All samples were tested up to 216 h till all samples showed evident signs of corrosion. In the first 24 h, white rusty corrosion products appeared on the surface of all samples pretreated with different technologies due to the corrosion of Zn coatings.

However, as the testing proceeds, red rusty corrosion products appear on the surface of samples due to the corrosion of substrates, which can reflect the anticorrosion properties of Zn coated NdFeB specimens pretreated with different technologies. The time for appearing red rusty corrosion products on the surfaces of samples with different pretreating technologies are 96 h for polishing, 144 h for pickling (50 s), 88 h for sandblasting and 132 h for the combined technology of sandblasting and pickling (5 s), respectively.

Fig. 9 shows SEM morphologies and EDS elemental compositions of Zn coated NdFeB specimens with different pretreatments after 132 h NSS test, (i) polishing, (ii) pickling (50 s), (iii) sandblasting and (iv) combined technology of sandblasting and pickling (5 s). Fig. 9(i) shows the SEM morphology of Zn coated NdFeB specimen with polishing pretreatment, and the top-right inset is the EDS elemental compositions. The smooth surface is produced by the polishing process. Low concentration of Zn element (9.6 wt%) shows the surface is mainly the corrosion products of the substrate,

and the Zn coating has been seriously corroded. The elemental ratios of Nd:Fe is 0.44:1, which is higher than that of the standard NdFeB substrate (~0.29:1), indicating the preferential corrosion of the Nd-rich phases. Fig. 9(ii) shows the SEM morphology of Zn coated NdFeB specimen with pickling (50 s) pretreatment. The unsmooth surface with microcracks and corrosion product of Zn can be observed. No Fe and Nd elements can be detected in the EDS pattern indicates the excellent anticorrosion properties of the Zn coating on the substrate with pickling pretreatment. Although the surface of the Zn coating on substrate pretreated by sandblasting technology is smoother with smaller microcracks than that of Zn coating on pickling substrate, 37.7 wt% Fe can be detected in the EDS pattern, as shown in Fig. 9(iii). Denser structure of the coating pretreated with sandblasting, as shown in Fig. 3(iii), results in the higher anticorrosion property of Zn coating. However, the existence of the Nd-rich phases in the substrate can be easily corroded when corrosion medium infiltrates from the microcracks of Zn coating. Also, the Nd:Fe elemental ratio 0.37:1 confirms the preferential corrosion of the Nd-rich phases. The combined technology of sandblasting and pickling (5 s) can result in the double effects of dense Zn coating and removal of Nd-rich phase in the surface layer of NdFeB substrate. Although little Fe (3.4%) can be detected in specimens pretreated with combined technology of sandblasting and pickling (5 s), as shown in Fig. 9(iv), which is much lower than that of polishing and sandblasting specimens. The anticorrosion properties of Zn coated NdFeB specimens pretreated with the combined technologies are much higher than that of specimens pretreated with polishing and sandblasting technologies, a little lower than that of pickling specimens.

The optical photographs of the Zn coated NdFeB specimens with different pretreating technologies after 168 h NSS test are shown in Fig. 10. Few red rusts can be observed on the surface of Zn coated samples pretreated with pickling and combined technology. However, most of the surfaces of polishing and sandblasting samples are covered with red rusts, indicating the serious corrosion of the substrates.

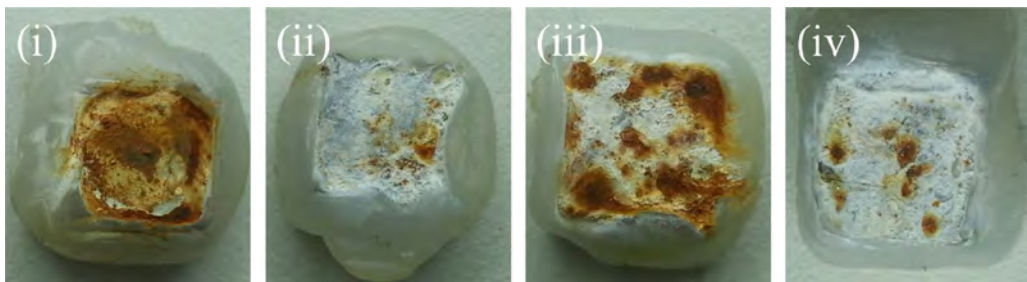


Fig. 10. Optical photographs of the Zn coated NdFeB specimens with different pretreatments after 168 h day NSS test, (i) polishing, (ii) pickling (50 s), (iii) sandblasting and (iv) combined technology of sandblasting and pickling (5 s).

The NSS results are consistent with that of the potentiodynamic polarization curves, which indicates that the Zn coated NdFeB specimens with pickling (50 s) and combined technology of sandblasting and pickling (5 s) pretreatments possess better corrosion resistance than that of samples with polishing and sandblasting pretreatments. The reason may be ascribed to the Nd-rich phases in intergranular regions.

The Nd-rich phase in intergranular regions possesses higher electrochemical activity than that of ferromagnetic matrix-phase ($\text{Nd}_2\text{Fe}_{14}\text{B}$) and Zn coating. When the aggressive medium permeated into the interface between the Zn coating and substrates, the preferred corrosion will take place in the Nd-rich phase due to the high electrochemical activity. And the galvanic corrosion occurs due to the existence of the potential difference between different phases [11]. If the surface only exists a ferromagnetic matrix-phase, the Zn coating can offer complete sacrificial anode protection due to its high electrochemical activity [39–41].

4. Conclusions

Different pretreating technologies were applied on NdFeB substrates for the following electroplating of Zn coatings. The adhesive strength between Zn coating and NdFeB substrate, and the anticorrosion properties were tested, and the mechanisms were discussed by measuring the morphologies, elemental compositions and the potentiodynamic polarization curves of the pretreated substrates.

The combined technology of sandblasting and pickling (5 s) achieves the highest adhesive strength between Zn coating and substrate and a high anticorrosion property (very close to the highest one pretreated by pickling (50 s)). The highest adhesive strength comes from the appropriate surface with higher surface roughness compared with polishing substrate, absence of loose layer compared with pickling (50 s) substrate and absence of broken particles compared with sandblasting substrate. The preferred dissolve of Nd-rich phases in the intergranular areas decreases the corrosion tendency of the substrates and the galvanic corrosion among Nd-rich phases, ferromagnetic matrix-phase and the Zn coating, hence, increase the anticorrosion property of Zn coated NdFeB specimens.

Acknowledgements

This work was financially supported by National Key Technology R&D Program of China (2012BAE02B01), the Natural Science Foundation projects of Anhui Province (1408085MKL72, 1408085MKL73), Anhui science and technology research projects (1301022080) and Dr. Special scientific research projects in Hefei University of technology (JZ2014HGBZ0333).

References

- [1] M. Sagawa, S. Fujimura, N. Togawa, H. Yamamoto, Y. Matsuura, *J. Appl. Phys.* 55 (1984) 2083–2087.
- [2] F. Vial, F. Joly, E. Nevalainen, M. Sagawa, K. Hiraga, K.T. Park, *J. Magn. Magn. Mater.* 242 (2002) 1329–1334.
- [3] J. Li, S. Mao, K. Sun, X. Li, Z. Song, *J. Magn. Magn. Mater.* 321 (2009) 3799–3803.
- [4] G. Bai, R.W. Gao, Y. Sun, G.B. Han, B. Wang, *J. Magn. Magn. Mater.* 308 (2007) 20–23.
- [5] D.F. Cygan, M.J. McNallan, *J. Magn. Magn. Mater.* 139 (1995) 131–138.
- [6] A.S. Kim, J.M. Jacobson, *IEEE Trans. Magn. Magn.* 23 (1987) 2509.
- [7] A. Saliba-Silva, R.N. Faria, M.A. Baker, I. Costa, *Surf. Coat. Technol.* 185 (2004) 321–328.
- [8] J.J. Ding, B.J. Xu, G.P. Ling, *Appl. Surf. Sci.* 305 (2014) 309–313.
- [9] J. Chen, B.J. Xu, G.P. Ling, Amorphous Al–Mn coating on NdFeB magnets: electrodeposition from AlCl_3 –EMIC– MnCl_2 ionic liquid and its corrosion behavior, *Mater. Chem. Phys.* 134 (2012) 1067–1071.
- [10] J. Xue, W. Zhao, G.K. Wolf, *Surf. Coat. Technol.* 187 (2004) 194.
- [11] L. Schultz, A.M. El-Aziz, G. Barkleit, K. Mummert, *Mater. Sci. Eng.* 267 (1999) 307–313.
- [12] A.A. El-Moneim, A. Gebert, *J. Appl. Electrochem.* 33 (2003) 795–805.
- [13] O. Filip, A.M. El-Aziz, R. Hermann, K. Mummert, L. Schultz, *Mater. Lett.* 51 (2001) 213–218.
- [14] C.L. Harland, H.A. Davies, *J. Alloys Compd.* 281 (1998) 37.
- [15] I. Skulj, H.E. Evans, I.R. Harris, *J. Mater. Sci.* 43 (2008) 1324–1333.
- [16] X. Yang, Q. Li, S. Zhang, H. Gao, F. Luo, Y. Dai, *J. Solid State Electrochem.* 14 (2010) 1601–1608.
- [17] C. Ma, X. Liu, C. Zhou, *J. Therm. Spray Technol.* 23 (2014) 456–462.
- [18] H. Zhang, Y.W. Song, Z.L. Song, *Mater. Corros.* 59 (2008) 324–328.
- [19] Y. Wang, Y. Deng, Y. Ma, F. Gao, *Surf. Coat. Technol.* 206 (2011) 1203–1210.
- [20] A. Walton, J.D. Speight, A.J. Williams, I.R. Harris, *J. Alloys Compd.* 306 (2000) 253–261.
- [21] I. Rampin, F. Bisaglia, M. Dabalà, *J. Mater. Eng. Perform.* 19 (2010) 970–975.
- [22] C.B. Ma, F.H. Cao, Z. Zhang, J.Q. Zhang, *Appl. Surf. Sci.* 253 (2006) 2251–2256.
- [23] S. Mao, H. Yang, J. Li, F. Huang, Z. Song, *Appl. Surf. Sci.* 257 (2011) 5581.
- [24] A. Ali, A. Ahmad, *Mater. Corros.* 60 (2009) 372–375.
- [25] A. Ali, A. Ahmad, K.M. Deen, *Mater. Corros.* 61 (2010) 130–135.
- [26] T.G. Woodcock, K. Khlopkov, A. Walther, N.M. Dempsey, D. Givord, *Scr. Mater.* 60 (2009) 826–829.
- [27] H. Yang, S. Mao, Z. Song, The effect of absorbed hydrogen on the corrosion behavior of sintered NdFeB magnet, *Mater. Corros.* 62 (2011) 122.
- [28] J.L. Xu, Z.X. Huang, J.M. Luo, Z.C. Zhong, Corrosion behavior of sintered NdFeB magnets in different acidic solutions, *Rare Metal Mater. Eng.* 44 (2015) 0786.
- [29] H.X. Yang, S.D. Mao, Z.L. Song, *Rare Metal Mater. Eng.* 40 (2011) 2241–2244.
- [30] J.Y. Yun, S. Ha, J.B. Lee, S.H. Kim, *Dent. Mater.* 7 (2010) 650–658.
- [31] J. Szewczenko, A. Zabuga, M. Kaczmarek, W. Kajzer, *Solid State Phenom.* 227 (2015) 463–466.
- [32] E. Lertora, C. Mandolino, C. Gambaro, *Key Eng. Mater.* 554 (2013) 996–1006.
- [33] B.N.J. Persson, M. Scaraggi, *J. Chem. Phys.* 141 (2014) 124701.
- [34] K. Meine, K. Klob, T. Schneider, D. Spaltmann, *Surf. Interface Anal.* 8 (2004) 694–697.
- [35] J. Takadoum, H.H. Bennani, *Surf. Coat. Technol.* 2 (1997) 272–282.
- [36] S.D. Mao, H.X. Yang, J.L. Li, H.G. Ying, Z.L. Song, *Vacuum* 85 (2011) 772–775.
- [37] Q.X. Qin, S.L. Liu, Adhesion of coating with substrate, *Plat. Finish.* 32 (2010) 0034.
- [38] J.L. Xu, Z.C. Zhong, Z.X. Huang, J.M. Luo, *J. Alloys Compd.* 570 (2013) 28–33.
- [39] F. Liu, Q. Li, X.K. Yang, Y. Dai, F. Luo, S.Y. Wang, H.X. Zhang, *Mater. Corros.* 62 (2011) 1141–1147.
- [40] S.D. Mao, H.X. Yang, Z.L. Song, J.L. Li, H.G. Ying, K.F. Sun, *Corros. Sci.* 53 (2011) 1887.
- [41] S.A. Attanasio, R.M. Latanision, *Mater. Sci. Eng., A* 198 (1995) 25.